DNA Binding Studies of Platinum(II) and Palladium(II) Complexes with Planar Tridentate 2,6-bis(N-R-benzimidazol-2-yl)pyridine Ligands

Abdurrahman Şengul*, Burak Coban, Pelin Türkoğlu, Burcu Tutkun

Department of Chemistry, Faculty of Arts and Sciences, Bulent Ecevit University, 67100 Zonguldak, Turkey

Abstract Four new complexes of platinum(II) and palladium(II) with planar tridentate ligands, 2,6-bis(*N*-H-benzimidazol-2-yl)pyridine (L-H), and 2,6-bis(*N*-methyl-benzimidazol-2-yl)pyridine (L-Me), as [Pt(L-H)Cl]Cl (**1**), [Pd(L-H)Cl]Cl (**2**), [Pt(L-Me)Cl]Cl (**3**), and [Pd(L-Me)Cl]Cl (**4**) have been synthesized and fully characterized by means of CHN, FT-IR (ATR), ^{1}H NMR, and ESI or MALDI TOF MS techniques. The DNA-binding behaviors of all complexes have been investigated by absorption titration, EtBr displacement measurement, and gel electrophoresis and viscosity measurement studies.

The results showed that complexes **1-4** can bind to DNA via partial intercalation mode. The metal complexes of L-Me, **3** and **4** are more hydrophobic, and thus showed better binding ability to DNA's hydrophobic environment, as revealed by the intrinsic binding constants K_b for **1-4** as being 4.76 ($\pm$ 0.6) x 10^4 M^{-1}, 5.01 ($\pm$ 0.9) x 10^4 M^{-1}, 2.50 ($\pm$ 0.6) x 10^5 M^{-1} and 2.25 ($\pm$ 0.9) x 10^5 M^{-1}, respectively. In addition, **3** and **4** are efficient cleavers of plasmid DNA.

Keywords Platinum; palladium; pyridine; benzimidazole; DNA binding

Introduction

Today, there is an enormous and growing interest in the chelating ligands and their transition metal complexes [1-3]. In particular, square-planar d^8 complexes of 2,6-bis(benzimidazol-2-yl)pyridine (bzimpy) ligands which act as moderate σ donor and π acceptor in comparison to structurally related and extensively studied tridentate 2,2′:6′,2″-terpyridine ligands [4, 5], have attracted great attention because of their photo-physical and intrinsic solid state properties [6-8], unique luminescent properties [9-11] and biological activities [12], such as molecular light switch for proteins [13].

The bis(benzimidazol-2-yl)pyridine ligands coordinate to metal center stronger than terpy because of more basic benzimidazole moieties [14, 15]. It is well known that substitution on terpy ligand can alter its reactivity, basicity and water solubility [16]. As shown in figure 1, the square-planar d^8 complexes of bzimpy derivatives incorporating N-H and N-methyl substituents should have different physical and electronic properties brought by the difference in basicity. Moreover, the steric effect of the ligands should lead to differences in solubility and aggregation tendency of the respective complexes, which are related to drug cytotoxicity, and also to potential interactions with DNA. It is known that DNA polyanionic strands have a significant affinity for the cationic Pt(II) and Pd(II) complexes of terpy [17]. In a related study on the DNA binding of [Zn(L)Cl$_2$] and [Hg(L)Cl$_2$] (L= bzimpy), no marked changes were observed in the electronic spectra of these labile complexes [18]. However, previous studies on the structural analogs complexes of the bidentate 2-(2′-pyridyl)benzimidazole with platinum(II) and palladium(II) have shown the Pt(II) complex to be significantly active *in vitro* against cell lines derived from human fibroblast Hs68 and certain brain tumors [19]. Later studies on these compounds have revealed that while dichloro-Pd(II) derivative shows modest activity towards human ovarian carcinoma cells (A2780) [20], the dichloro-Pt(II) derivative [21] shows

activity *in vitro* against the human rhabdomyosarcoma cell line. Remarkably, the complex ion [Pt(bzimpy)Cl]$^{+}$ was found to be able to bind to Cys104 in the subunit C of hemoglobin [13]. In addition, [Pt(bzimpy)Cl]$^{+}$ was reported to bind to c-*myc* G-quadruplex DNA structure in a cell-free system [22]. Although, palladium(II) and platinum(II) adopt the same square-planar geometry and display the similar characteristics when coordinated to N-donor ligands, they have different ligand-exchange kinetics during the aquation reaction (Pd^{II} is 10^{6} times faster than Pt^{II} as estimated) [23]. A study on the G-quadruplex-DNA binding properties of the Pt(II) and Pd(II) complexes of analogous 2,2'-(4-*p*-tolypyridine-2,6-diyl)*bis*-1-methyl-benzimidazole has revealed a greater ability of the palladium complexes to coordinate DNA bases, and thus to inhibit the growth of cancer cells (KB, A549 and MCF7) more efficiently than their platinum(II) counterparts [24]. As demonstrated by the previous studies, the DNA affinity, the binding mode and the strength of the metal complexes can be modulated by modifying either the metal ion or the organic ligand. Therefore, we have modulated both the ligand (N-H and N-Me derivatives) and the coordinating metal ion (figure 1) to study *in vitro* activity of these complexes with tridentate bzimpy ligands. Here we report the syntheses and characterization of **1-4** (figure 2). In addition, the comparative DNA-binding properties have been investigated by absorption and emission methods as well as by viscosity measurements. The DNA-cleavage behaviors of the complexes towards pBR322 were also investigated.
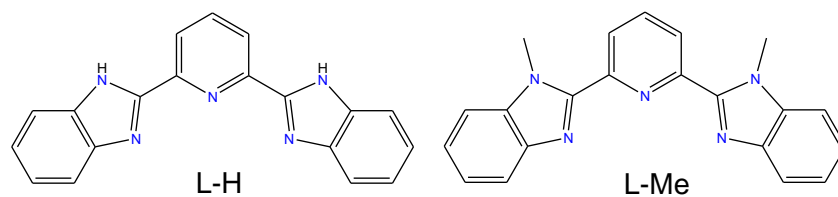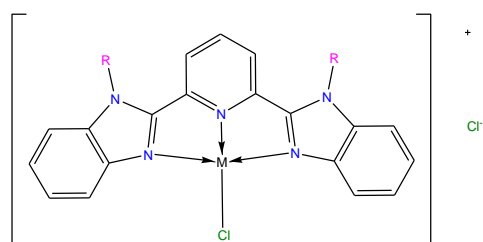

Figure 1: Molecular structures of the tridentate N-donor ligands

Complex	M	R
1	Pt(II)	H
2	Pd(II)	H
3	Pt(II)	CH$_3$
4	Pd(II)	CH$_3$

Figure 2: Chemical structures of the metal complexes

Materials and Methods

All reagents and solvents were of commercial origin and used without further purification unless otherwise noted. The starting compounds, [Pt(DMSO)$_2$Cl$_2$] and [Pd(DMSO)$_2$Cl$_2$] were synthesized as reported [25]. Solutions of calf thymus DNA (CT-DNA; purchased from Sigma) in 50 mM ammonium acetate (pH 7.5) had a UV−vis absorbance ratio of 1.8–1.9: 1 at 260 and 280 nm (A260/A280 = 1.9), indicating that the DNA was sufficiently free of a protein [26]. The concentration of DNA was determined spectrophotometrically using a molar absorptivity of 6,600 M^{-1} cm^{-1} (260 nm) [26]. Double-distilled water was used to prepare buffers. The stock solution of ct-DNA was stored at 4 °C and used within 4 days of preparation. Solutions of the Pt(II) and Pd(II) complexes were prepared by dissolving a weighed amount in 0.5 mL DMSO for solubility reasons and were subsequently diluted (up to 150 times without precipitation) with 50 mM ammonium acetate (pH 7.5) to the required concentration.

Physical Measurements

Microanalyses (C, H, and N) were performed with Leco 932 CHNS analyzer. FT-IR spectra were recorded with a PerkinElmer Spectrum 100 instrument. ^{1}H NMR spectra were recorded with a Bruker Ultra Shield Plus ultra-long-hold-time spectrometer with $(CD_3)_2SO$ or $CDCl_3$ as the solvent for the ligands, $(CD_3)_2SO$ as the solvent for the complexes, and tetramethylsilane as an internal standard at 400 MHz at room temperature. All chemical shifts are given relative to tetramethylsilane. The ESI-MS measurements were carried out by AB SCIEX 4000 Q TRAP, melting points were determined by BÜCHI Melting point B-540, gel electrophoresis were measured with Thermo Electron Corporation EC-330 Midicell Primo, UV–Vis spectra were recorded on a Varian Cary 100 spectrophotometer and emission spectra were recorded with a PerkinElmer LS 55 spectrofluorophotometer at room temperature.

Synthesis

Preparation of 2,6-bis(NH-benzimidazol-2-yl)pyridine, L-H: The ligand was synthesized according to previously published procedures [27, 28] for analogs compounds, as follows. Polyphosphoric acid (PPA) was heated at elevated temperature to obtain a viscous shrub. Next, 1,2-phenylenediamine (2.0 equiv.) and 2,6-pyridine dicarboxylic acid (1.0 equiv.) was added and the solution was set to reflux for 4 h. The solution was allowed to stand at room temperature and then poured into a 100 mL of ice-cold water. The green precipitate was filtered and neutralized with a concentrated Na_2CO_3 solution. The crude solid was recrystallized from methanol to yield a white crystalline product. Yield: 82%, m.p.: 350 °C, ESI-MS: m/z = 312.1 [M$^+$] (figure S1). Anal. Calcd for $C_{19}H_{13}N_5$: C, 73.30; H, 4.21; N, 22.49. Found: C, 73.2; H, 4.4; N, 22.1 (%). ^{1}H NMR (400 MHz, DMSO-d_6, δ, ppm): 13.0 (2H, s), 8.35 (2H, d, J = 7.73 Hz), 8.17 (1H, m), 7.77 (4H, m), 7.33 (4H, m) (figure S2). FT-IR (v, cm^{-1}): 3140 (C-H$_{ar}$), 1574 (C = N), 1458, 1437 (C = C$_{ar}$) (figure S3).

Preparation of 2,6-bis(N-methyl-benzimidazol-2-yl)pyridine, L-Me: This compound was synthesized in the same manner with the exception of using N-methyl-1,2-phenylenediamine. Yield: 80%, m.p.: 190 °C. ESI-MS: m/z = 339.0 [M + H]$^+$ (figure S4). Anal. Calcd for $C_{21}H_{17}N_5$: C, 74.32; H, 5.05; N, 20.63. Found: C, 74.2; H, 5.2; N, 21.1(%). ^{1}H NMR (400 MHz, DMSO-d_6, δ, ppm):): 8.40 (2H, d, J = 7.83), 8.21 (1H, m), 7.78 (2H, d, J = 7.71), 7.70 (2H, d, J = 7.88), 7.34 (4H, m), 4.26 (6H, s) (figure S5). FT-IR (v, cm^{-1}): 3050 (CH$_{ar}$), 2976, 2938 (CH$_{al}$, N-CH$_3$), 1568 (C = N), 1483, 1472 (C=C) (figure S6).

Preparation of [Pt(L-H)Cl]Cl·2H$_2$O (1): The ligand L-H (1.0 equiv.) was added to the solution of [Pt(DMSO)$_2$Cl$_2$] [25, 29] (1.0 equiv.) in dichloromethane (50 mL) with vigorous stirring at r.t. and set to reflux for 6 h. The orange precipitate was obtained after evaporation of the solvent under vacuum. After washing with plenty of diethyl ether, it was vacuum-dried. Yield: 78%. ESI-MS: m/z = 577 [M-Cl+H]$^+$; (figure S7). Anal. Calcd for $C_{19}H_{17}N_5Cl_2O_2Pt$: C, 37.21; H, 2.79; N, 11.42. Found: C, 37. 1; H, 2.9; N, 11.5(%). ^{1}H-NMR (400 MHz, CDCl$_3$, δ, ppm): 13.2 (2H, s), 8.50 (2H, d, J = 7.75), 8.25 (1H, m), 7.80 (4H, m), 7.40 (4H, m) (figure S8). FT-IR (ATR) (v, cm^{-1}): 3433(NH), 3369 (H$_2$O), 3048 (C-H$_{ar}$), 1571 (C=N), 1477, 1439 (C=C$_{ar}$) (figure S9).

Preparation of [Pd(L-H)Cl]Cl·2H$_2$O (2): The orange color complex was synthesized in the same manner, by using Pd(DMSO)$_2$Cl$_2$ [25]. Yield: 97%. MALDI-TOF MS: m/z = 450.6 [M+H]$^+$ for [Pd(L-H)Cl]$^+$ (figure S10). Anal. Calcd for $C_{19}H_{17}N_5Cl_2O_2Pd$: C, 43.49; H, 3.27; N, 13.35. Found: C, 43.4; H, 3.5; N, 13.2(%). ^{1}H NMR (400 MHz, CDCl$_3$, δ, ppm): 12.9 (2H, s), 8.43 (2H, d, J = 7.50), 8.20 (1H, m), 7.75 (4H, m), 7.40 (4H, m) (figure S11). FT-IR (ATR) (v, cm^{-1}): 3383 (N-H), 3250-3125 (H$_2$O), 3040 (C-H$_{ar}$), 1575 (C=N), 1455, 1438 (C=C$_{ar}$) (figure S12).

Preparation of [Pt(L-Me)Cl]Cl·CH$_3$OH (3): The ligand, L-Me (1.0 equiv.) was added drop-wise to the solution of Pt(DMSO)$_2$Cl$_2$ in methanol, and then set to reflux for 6 h. After evaporation of the solvent under reduced pressure, the obtained orange solid was washed with plenty of diethyl ether and vacuum-dried. Yield: 72%. ESI MS: m/z = 450.6 [M-Cl+H]$^+$ for [Pt(L-Me)Cl]+CH$_3$OH (figure S13). Anal. Calcd for $C_{22}H_{21}N_5Cl_2OPt$: C, 41.45; H, 3.32; N,

10.99. Found: C, 41.4; H, 3.5; N, 10.8(%). ^{1}H NMR (400 MHz, DMSO-d_6, δ, ppm): 8.40 (2H, d, J = 7.83), 8.20 (1H, m), 7.76 (2H, d, J = 7.71), 7.69 (2H, d, J = 7.88), 7.36 (2H, m), 7.30 (2H, m), 4.26 (6H, s) (figure S14). FT-IR (ATR) (ν, cm^{-1}): 3297(OH), 3092, 3022 (C-Har), 2907, 2871 (N-CH$_3$), 1604, 1589, 1537 (C=N), 1484, 1456 (C=C) (figure S15).

Preparation of [Pd(L-Me)Cl]Cl·2H$_2$O (4): The orange color complex was synthesized in the same manner, by using Pd(DMSO)$_2$Cl$_2$ Yield: 72%. ESI MS: m/z = 480.0 [M-Cl+H]$^+$ for [Pd(L-Me)Cl]$^+$ (figure S16). Anal. Calcd for C$_{21}$H$_{21}$N$_5$Cl$_2$O$_2$Pd: C, 45.63; H, 3.83; N, 12.67. Found: C, 45.5; H, 3.8; N, 12.8(%). ^{1}H NMR (400 MHz, DMSO-d_6, δ, ppm): 8.58 (2H, d, J = 7.79), 8.40 (1H, m), 7.40 (2H, d, J = 7.70), 7.23 (2H, d, J = 7.76), 7.09 (2H, m), 6.95 (2H, m), 3.83 (6H, s) (figure S17). FT-IR (ATR) (ν, cm-1): 3398 (H$_2$O), 3125 (C-Har), 2941, 2879 (N-CH$_3$), 1601, 1586, 1572, 1534 (C=N), 1493, 1483, 1462 (C=C) (figure S18).

Absorption and emission titrations

For the absorption and emission titrations, complexes were dissolved in a minimum amount of DMSO, and were then diluted in buffer (5 mM ammonium acetate, pH 7.5) to a final concentration of 20 μM. Titrations were performed in a 10-mm stoppered quartz cell by using a fixed concentration of the complex (20 μM), to which the CT-DNA stock solution was added in the increments of 1 μL to a DNA-to-the complex concentration ratio of 6:1. The analysis was performed by with UV–Vis or fluorescence spectrophotometer by recording the spectrum each time DNA was added. Complex–DNA solutions were incubated for 10 min each time before the spectra were recorded. A control solution of 20 μM complex in the same buffer was treated in the same manner. Cell compartments were thermostated at $25 \pm 0.1°$C.

For emission intensity measurements, the excitation wavelength was fixed and the emission range was adjusted before the measurements. Ammonium acetate (5 mM), pH 7.5 buffer was used as a blank to make preliminary adjustments. All measurements were performed with a 5-nm entrance slit and a 5-nm exit slit. The complexes were excited at 370; the emission spectra were monitored at 650 and 740 nm. Quenching studies were carried out for complexes **3** and **4** with the anionic quencher potassium iodide (KI).

Competitive Studies

We used fluorescence spectroscopy in order to examine whether each complex was able to displace ethidium bromide (EB) from the DNA–EB adduct. DNA was pretreated with EB at a DNA-to-EB concentration ratio of 50:1 for 30 min at 27 °C to prepare the initial DNA-EB adduct. The intercalating effect of the complexes with the DNA-EB complex was studied by adding a certain amount of a solution of the complex in increments to the solution of the DNA-EB complex. The influence of each addition of complex to the solution of the DNA-EB adduct was obtained by recording the change in the fluorescence spectrum. To study the competitive binding of the complexes with EB, EB was excited at 453 nm in the presence of DNA alone as well as in the presence of the complexes.

We examined whether **3** is able to displace TO from the DNA-TO adduct. DNA was pretreated with thiazole orange (TO) at the TO to DNA concentration ratio of 2:1 for 30 min at 27 °C to prepare the initial DNA-TO adduct. The intercalating effect of **3** was studied by adding, in increments, a certain amount of the compound solution to the solution of the DNA-TO adduct. TO was excited at 504 nm.

Viscosity Measurements

Viscosity measurements were performed using a common Ubbelohde viscometer maintained at a constant temperature of 30.0 ± 0.1 °C (in a thermostatic bath). The DNA concentration was 160 μM. The flow time was measured with a digital stopwatch; every sample was measured three times and an average flow time was calculated. Data are presented as $(\eta/\eta_0)^{1/3}$ versus binding ratio, where η is the viscosity of DNA in the presence of the complex and η_0 is the viscosity of DNA alone.

DNAse Activity by Gel Electrophoresis

Gel electrophoresis experiments were performed using pBR322 negatively supercoiled plasmid DNA and 1% agarose gels together with a tris(hydroxymethyl)aminomethane-borate-EDTA running buffer solution. Reaction mixtures (10 mL) containing 0.1 μg pBR322 together with different amounts of **1** to **4** (0, 30, 60, 90, 120, 150 and 180 μM) in 50 mM ammonium acetate buffer, pH 7.5 were prepared at 0 °C. They were next incubated at 36 °C for 1 h in the dark. Prior to loading samples in the gel, 2.5 mL of 0.25% bromophenol blue loading buffer and sucrose in water (40% w/v) was added to the mixture. Gels were obtained at room temperature by using a Thermo midi horizontal agarose gel electrophoresis system at 35 V for 4 h. The resulting gels were stained with EB solution (0.5 mg mL^{-1}) for 45 min, after which they were soaked in water for a further 20 min. Gels were visualized under UV light and photographed.

Results and Discussion

Synthesis of the Ligands and Complexes

The ligands L-H and L-Me were synthesized by the well-established procedure [27, 28]. The structures of the compounds were confirmed by CHN analyses, ESI-MS, FTIR (attenuated total reflection) spectroscopy, and ^{1}H NMR spectroscopy. The chemical and spectroscopic data are identical with the literature data for the same ligands [9, 30, 31]. In the ^{1}H NMR spectra of L-H and L-Me, the protons in the pyridine ring are observed as doublet and multiplet in 2:1 ratio at around 8.40-8.17 ppm. The L-H displays a singlet at 13.0 ppm assigned to the N–H of the imidazole groups, while the observed singlet at 4.26 ppm for L-Me assigned to the N-methyl groups on the imidazole rings [30]. The protons of the benzimidazole rings of the each ligand appear as multiplets at around 7.78-7.33 ppm. The infrared spectra of L-H and L-Me are very similar with the exception of the observed aliphatic CH stretching band at 2976 and 2938 cm^{-1} for L-Me due to N-methyl groups, respectively. The corresponding metal complexes with Pt(II) and Pd(II) were synthesized by mixing the ligand with [Pt(DMSO)$_2$Cl$_2$] or [Pd(DMSO)$_2$Cl$_2$] in an equimolar ratio in DCM or methanol to yield the solvated (methanol or water) complexes as described in the experimental section. The reactions resulted in a pure crystalline product, which can be easily purified by recrystallization. The purity of the complexes was carefully checked by elemental analysis, ^{1}H NMR as well as ESI-MS or MALDI-TOFF MS spectra. The molecular structures were also further supported by FT-IR spectroscopy. The IR spectrum of the each complex is almost identical to the corresponding ligand. The ^{1}H NMR spectra of the complexes show some differences from their respective ligands, especially pronounced for the pyridine protons. The protons at the *meta*-positions in pyridine (H^{3} and H^{5}) are more affected by complexation formation with the metal cation, and thus undergo deshielding, for example, the doublet assigned to the py-H^{3}, H^{5} protons appear at 8.35 and 8.40 ppm for L-H and L-Me, respectively, whereas for the respective metal complexes, they appear at 8.50, 8.43, 8.40 and 8.58 ppm for **1**-**4**, respectively. The chemical shifts of the ligands and the corresponding Pt(II) and Pd(II) complexes are comparable to those reported in the literature [7, 22, 32, 33]. The different degree or variation of deshielding of the py protons upon coordination to the metal ion may due to the tendency of these square-planar complexes to aggregate in solution and in the solid state [6, 7, 9]. The chemical analysis showed that all complexes contain the solvent of crystallization as revealed by the CHN and ESI-MS or MALDI-TOFF MS analysis (see experimental section).

Electronic Absorption Titration

Examining electronic spectra is a useful method to investigate the interactions of complexes with DNA. A complex bound to DNA through external binding or groove binding usually results in hyperchromism, while binding through intercalation usually results in hypochromism and red shift owing to the intercalation mode involving a strong stacking interaction between an aromatic chromophore and the DNA base pairs. The extent of the hypochromism or hyperchromism in the visible metal-to-ligand charge transfer band is commonly consistent with the strength of the interaction [34].
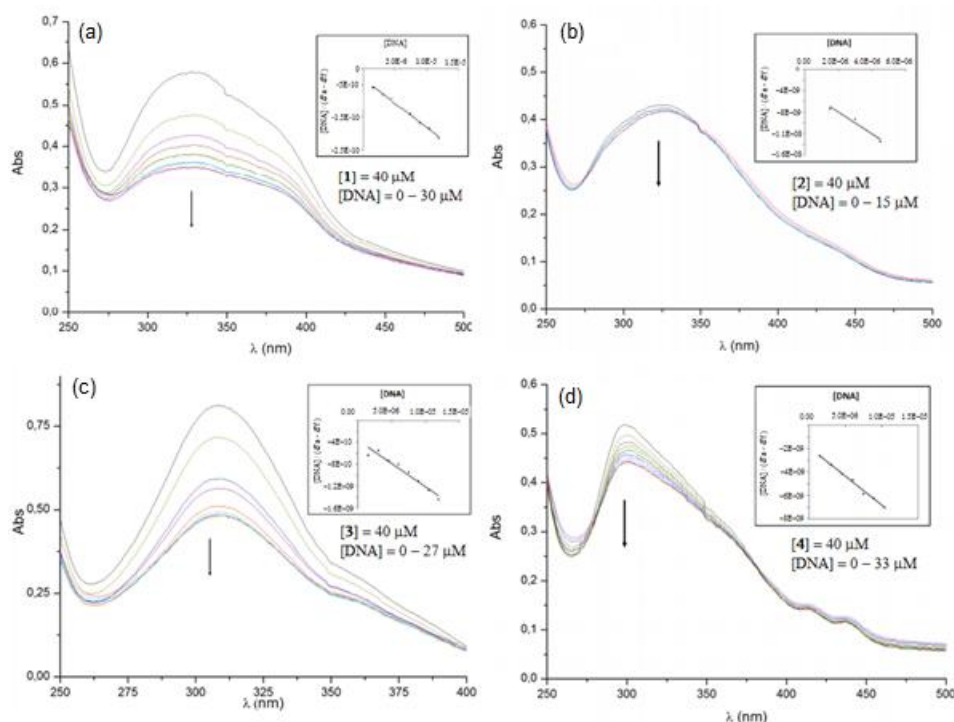
*Figure 3: Absorption spectra of **1-4**, respectively in (a), (b), (c), (d) in 50 mM ammonium acetate buffer on the addition of calf thymus DNA: 20 μM complex, 0–64 μM DNA. Arrows show the absorbance changing with the increase of DNA concentration. The insets show plots of DNA concentration divided by the difference between the apparent absorption coefficient (ε_A) and the absorption coefficient of the free platinum complex (ε_f) versus DNA concentration for the titration of DNA to Pt(II) complexes.*

The absorption spectra of the complexes in the absence and presence of CT-DNA (at a constant 20 μM concentration of the complexes) are shown in figure 3. After increasing DNA concentration, the hypochromism was present, although we did not observe any obvious red shift in the metal-to-ligand charge transfer band of the complexes **1-4**. When the amount of DNA was increased, the intensities of the π-π* transitions decreased as follows: 40% for **1**, at a DNA-to-Metal concentration ratio of 0.4, 10% for **2** at a DNA-to-Metal concentration ratio of 0.2, 40% for **3**, at a DNA-to-Metal concentration ratio of 0.35, and 15% for **4** at a DNA-to-Metal concentration ratio of 0.6. For quantitative comparison of the DNA-binding affinities, the intrinsic binding constants K_b of the complexes were measured by monitoring the changes in the π-π* absorbance at around 330 for **1** and **2** and 315 nm for **3** and **4**, according to the following equation (1):

$$[DNA]/(\varepsilon_A - \varepsilon_f) = [DNA]/(\varepsilon_B - \varepsilon_f) + 1/K_b(\varepsilon_B - \varepsilon_f) \tag{1}$$

where [DNA] is the nucleic acid concentration in base pairs, ε_A is the apparent absorption coefficient obtained by calculating A_{obs}/[complex], and ε_f and ε_B are the absorption coefficients of the free and the fully bound platinum complex, respectively. In the [DNA]/($\varepsilon_A - \varepsilon_f$) versus [DNA] plot, K_b is given by the ratio of the slope to the intercept. The values of the intrinsic binding constants K_b for complexes **1-4** were derived to be 4.76 ($\pm$ 0.6) x 10^4 M^{-1}, 5.01 ($\pm$ 0.4) x 10^4 M^{-1}, 2.50 ($\pm$ 0.6) x 10^5 M^{-1} and 2.25 ($\pm$ 0.3) x 10^5 M^{-1}, respectively. When the complexes are putted in order according to their K_b values, the result is **3 > 4 > 1 > 2**. These values are comparable to those of complexes such as [Co(bzimpy)$_2$]$^{2+}$ (K_b = 1.6 x 10^5 M^{-1}) [35], [Zn(bzimpy)NO$_3$]$^+$ (K_b = 6.5 x 10^5 M^{-1}) [36], [Pt(terpy)Cl]$^+$ (K_b = 1.3 x 10^5 M^{-1}) and [Pd(terpy)Cl]$^+$ (K_b = 1.9 x 10^5 M^{-1}) [37], higher than [Cu(bzimpy)(bipy)H$_2$O]$^{2+}$ (K_b = 1.41 x 10^4) and [Cu(bzimpy)(en)H$_2$O]$^{2+}$ (K_b = 1.32 x 10^4 M^{-1}) [38], [Cr(bzimpy)$_2$]$^+$ (Kb = 1.0 x 10^4 M^{-1}) [39], [Cu(bzimpy)Cl]$^+$ (K_b = 1.8 x 10^4 M^{-1}) [40], [Ru(bzimpy)(bipy)]$^{2+}$ (K_b = 3.6 x 10^4 M^{-1}) [41], [Pt(py)(terpy)]$^{2+}$ (K_b = 3.5 x 10^4 M^{-1}) [42], but lower than classical intercalator [Ru(dppz)(bpy)$_2$]$^{2+}$ (dppz is dipyridophenazine) (K_b = 5.0 x 10^6 M^{-1}) [43]. It is

therefore clear that the complexes **1-4** intercalate less strongly into the DNA base pairs than the classical intercalators.

Notably, the resonance-stabilizing electron-donating substitution in benzimidazole ring of **3** was shown to increase ct-DNA binding affinity up to 5-fold relative to **1** which has an unsubstituted imidazole ring system. Because methyl substituted benzimidazole ring is more hydrophobic, the ligand may intercalate easier into the hydrophobic interior of ct-DNA. This can also explain the larger binding affinity of **3** to ct-DNA in comparison to **1**. On the other hand, the DNA binding affinities of Pt(II) and Pd(II) are very similar, which suggests that the type of metal ion in the complex did not play a significant role in this case.

Emission Spectra

In the absence of DNA, complexes **1-4** can emit weak luminescence in ammonium acetate buffer at ambient temperature, with the maximum at 674 nm (**1**), 692 nm (**2**), 688 nm (**3**) and 644 nm (**4**). On addition of ct-DNA, the emission intensity of each complex slightly increases (figure S19) as reported for $[Zn(bzimpy)NO_3]^+$ [36], $[Cr(bzimpy)_2]^+$ [39], $[Cu(bzimpy)(bipy)H_2O]^{2+}$ and $[Cu(bzimpy)(en)H_2O]^{2+}$ [38], $[Ru(bzimpy)(bipy)(H_2O)]^{2+}$ and $[Ru(bzimpy)(phen)(H_2O)]^{2+}$ complexes [41]. This implies that the complexes can interact with ct-DNA and are efficiently protected by DNA, since the hydrophobic environment inside the DNA helix reduces the accessibility of solvent water molecules to the complex and the mobility of the complex is restricted at the binding site. This leads to a decrease in the vibrational modes of relaxation. The amount of increase that we observed is, however, less than that observed for classical intercalators. Among the complexes **1-4**, the highest increase of 55% was achieved by **3**, indicating the strongest interaction with DNA.

Control Fluorescence Quenching by KI

Quenching experiments indicate the location of the bound complex to DNA. An anionic quencher would quench the fluorescence intensity of the complex bound to the surface of the helix. However, if the complex is intercalated, then little or no change in its fluorescence is expected. The fluorescence intensities of the complexes were quenched by the iodide anion in the absence of DNA (figure S20). The quenching was harder when the DNA was present. This can be explained by repulsion of the negative anion from DNA polyanion which prevents the access of the iodide to the intercalatively bound complex. However, the strength of the binding is not as strong as the classical intercalators. As shown in figure S20, the quenching protection is higher for the complexes, **3** and **4** compared to the complexes **1** and **2**. Based on the slope to the intercept ratio (figure S20), the ct-DNA binding strengths are higher for the complexes **4** and **3** than for **1** and **2**, similar to the results of the absorption spectroscopy: **4 = 3 > 1 = 2**.

Competitive Binding Experiments

Competitive binding experiments with a well-established quenching assay based on the displacement of the intercalating compound EB from ct-DNA may give further information regarding the DNA-binding properties of the complex. A complex which is involved in strong DNA intercalation would compete with EB for the DNA binding and quench the EB emission. When a complex displaces EB from DNA-bound EB, its fluorescent emission greatly quenched since free EB molecules are readily quenched by the surrounding water molecules [44]. DNA intercalators were reported to cause an evident reduction in EB emission intensities [45], but only moderate decrease in emission intensities were reported for DNA groove binders [46, 47]. The degree of binding of the complexes can be calculated by the Stern–Volmer equation (2) [48].

$$I_0/I = 1 + Kr \tag{2}$$

where I_0 and I represent the fluorescence intensities in the absence and presence of the complex, respectively, K is a linear Stern–Volmer quenching constant dependent on the ratio of the concentration of bound EB to the concentration of DNA, and r is the ratio of the total concentration of the complex to the concentration of DNA. As shown in figure 4, an appreciable reduction in emission intensity was achieved by the addition of **1** to the EB–DNA system. None of the complexes has quenched the emission intensity of EB-DNA system by 50%; therefore the binding constants were not calculated.
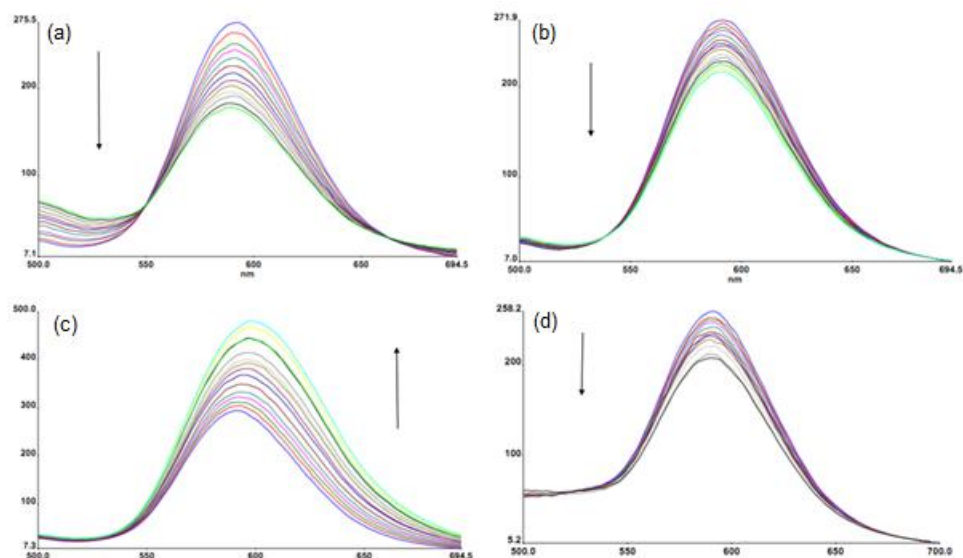
*Figure 4: Emission spectra of ethidium bromide bound to DNA in the presence of **1-4**, respectively in (a), (b), (c), (d) (0.0–92.0 μM). The arrows show the intensity changes on increasing the concentration of the complex*

Predictably, the performance of **3** is higher than that of **1**. Instead, the emission of EB-DNA system was increased by the addition of **3**, due to the unexpected emission band at the same wavelength. To further investigate this phenomenon, thiazole orange (TO), i.e. another compound known for its DNA-intercalating property, was used in place of EB in the competition experiment. This experiment (figure 5) showed that **3** completely quenched the emission intensity of TO-DNA system, indicating that **3** has replaced TO in the DNA bound complex as an intercalator [49].
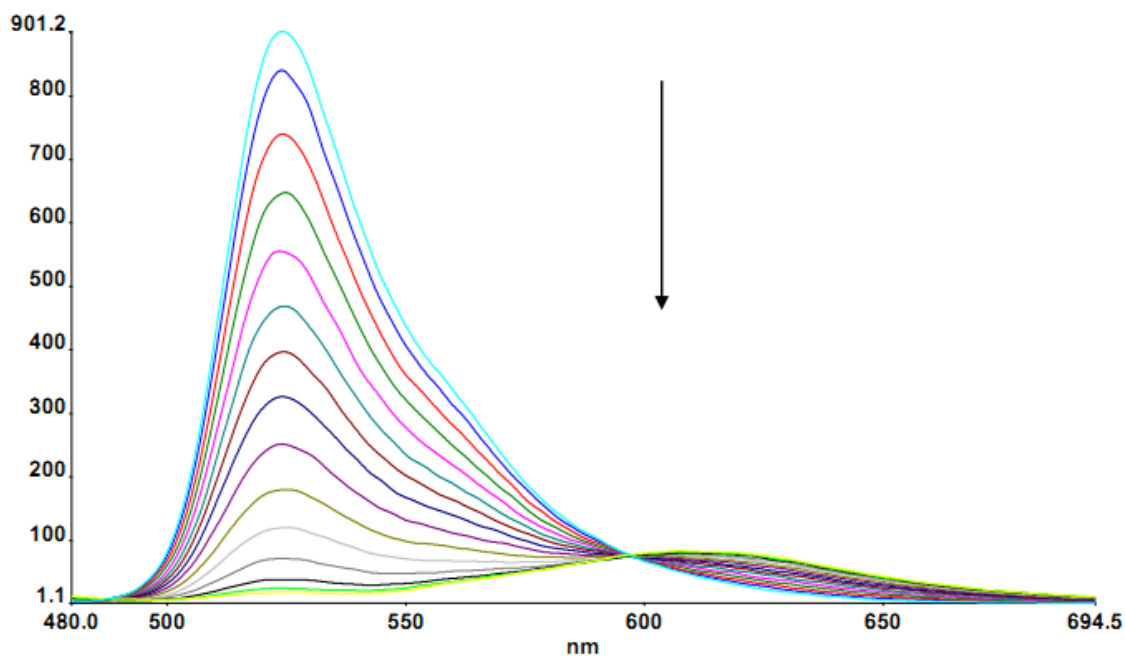

*Figure 5: Emission spectra of thiazole orange (TO) bound to DNA in the presence of **3** (0.0–92.0 μM). The arrows show the intensity changes on increasing the concentration of the complex*

Viscosity Properties

Hydrodynamic measurements (*i.e*., viscosity and sedimentation), being sensitive to length changes, are regarded as the least ambiguous and most critical tests in solution for a classic intercalation model when the crystallographic structural data are absent. A classic intercalation model demands that the DNA helix increases in length as base pairs are separated to accommodate the bound ligand. This leads to an increase in DNA viscosity. In contrast, a partial, non-classic intercalation of a ligand could bend (or kink) the DNA helix, reducing its length and, concomitantly, its viscosity [50]. The effects of **1-4** and EB on the viscosity of rod like DNA are shown in figure 6. For EB, the proven classic intercalator will exert the maximum effect on the viscosity of DNA. By increasing the amount of the complexes, the relative viscosity of DNA increases steadily indicating that the complexes bind to DNA via partial intercalation. The comparative extent of the increase in viscosity, which may depend on the DNA-binding affinity, follows the order EB > **4** = **3** > **2** = **1**. This is consistent with the spectroscopic results described earlier. The complexes of the same ligands alter the viscosity of CT-DNA in the same order independent of the metal ion.
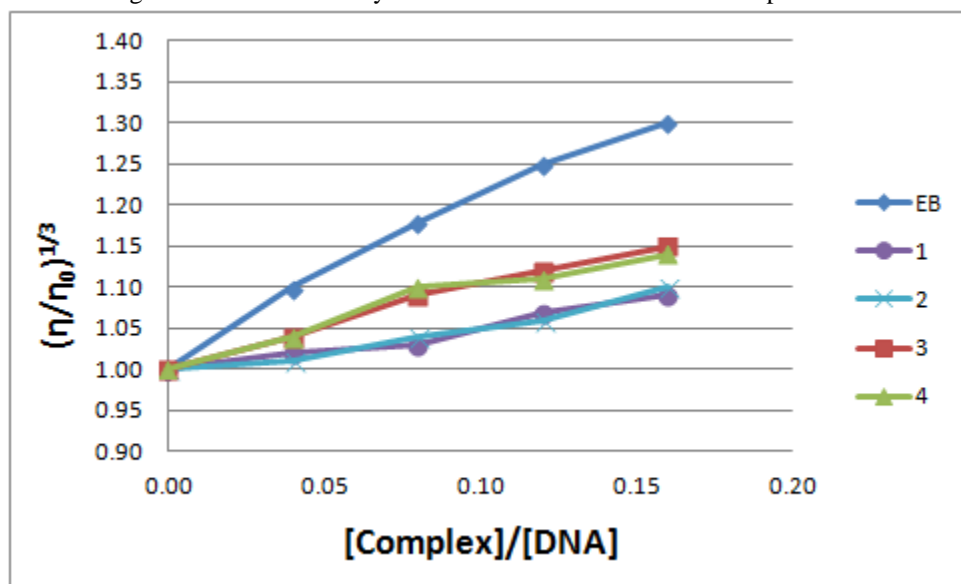

*Figure 6: Effects of increasing amounts of ethidium bromide (EtBr; blue diamonds) and **1-4**, on the relative viscosity of calf thymus DNA at (25 ± 0.1) °C. The total concentration of DNA is 0.5 mM*

Cleavage of pBR322 DNA by Complexes

The potential of the present complexes to cleave DNA was studied by gel electrophoresis using supercoiled pBR322 DNA in ammonium acetate buffer (pH 7.5). When circular plasmid DNA is subjected to gel electrophoresis, relatively fast migration should be observed for the intact supercoiled form (form I). If scission occurs on one strand only (nicked circular), the supercoiled form will relax to generate a slower-moving open circular form (form II). If both strands are cleaved, a linear form (form III) that migrates between forms I and II is generated [34]. The separation of pBR322 DNA by gel electrophoresis after incubation with each complex (**1-4**) is shown in figure S21. Increasing concentrations of **1** and **2** result in no change in the intensity of form I when compared with the control (lane 1). At high concentrations of **3** and **4**, DNA cleavage seems to be so extensive that both forms of pBR322 disappear from the agarose gel [51-53]. Control experiments were carried out in the presence of a singlet oxygen quencher (NaN₃) and free radical scavenger (dimethyl sulfoxide, (DMSO)) [54]. As shown in figure 7, azide (lane 5) inhibited to some extent, indicating the involvement of a singlet oxygen, and the hydroxyl scavenger DMSO (lane 6) reduced the nuclease activity which is indicative of the involvement of the (•OH) hydroxyl radical in the cleavage activity of the Pt(II) complex (**3**). For the cleavage activity of Pd(II) complex (**4**), azide ions (lane 5) completely inhibited cleavage indicating that the singlet oxygen was involved in the nuclease activity, whereas DMSO (lane 6) had no inhibitory effect. The nuclease activity of **3** and **4** was not completely diminished in the presence of the

singlet oxygen quencher and free radical scavenger. This means that DNA was cleaved by a mechanism other than oxidation, possibly a hydrolytic path.
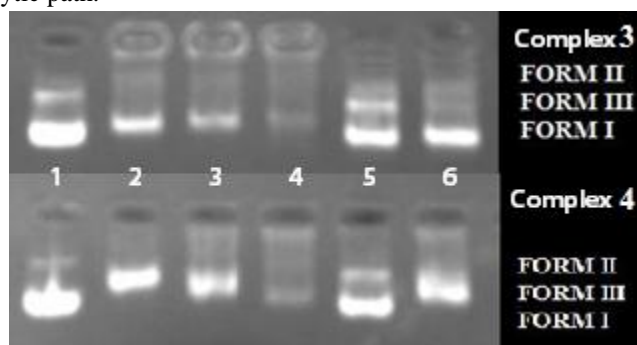

Figure 7: Cleavage of pBR322 DNA by 3 and 4 in the presence of H$_2$O$_2$ (30 mM) in the buffer. Lane 1, DNA alone; lanes 2–4, DNA was incubated for 1 h with increasing concentrations of the complexes (40, 60 and 90 µM); lane 5 and 6: 20 µM complex, H$_2$O$_2$ and the addition of radical scavengers NaN$_3$ and DMSO, respectively.

Conclusion

Four new complexes **1-4** have been synthesized and fully characterized. The DNA-binding affinities and DNAse activities of these complexes have been investigated. The results showed that complexes **1-4** can bind to DNA but with different affinities. The DNA binding affinities depend on the ligand type but are independent of which the metal ion (Pd(II) or Pt(II)) is present in the complex, as revealed by the similar binding constants of **1** and **2** incorporating L-H ligand (K_b = 4.76 (± 0.6) x 10^4 M^{-1} and 5.01 (± 0.9) x 10^4 M^{-1}, respectively), and **3** and **4** incorporating L-Me ligand (K_b = 2.50 (± 0.6) x 10^5 M^{-1} and 2.25 (± 0.9) x 10^5 M^{-1}, respectively). The methylated benzimidazole nitrogen makes **3** and **4** more hydrophobic and so results in better binding ability to DNA's hydrophobic environment. Because the classical intercalators have much higher binding constants, a slight increase in the viscosity of DNA upon addition of the complexes, as well as the results of the fluorescence quenching experiments suggest that the complexes bind DNA *via* partial intercalation. In addition, **3** and **4** are efficient cleavers of plasmid DNA, possibly *via* a hydrolytic pathway.

Supplementary Data

Supplementary data (FT-IR, ^{1}H NMR and ESI-MS or MALDI-TOFF mass and absorption and emission spectra of the compounds associated with this article (figure S1-figure S21) are provided.

Acknowledgments

References

1. Eryazici, I, Moorefield, CN, Newkome, GR. Square-planar Pd(II), Pt(II), and Au(III) terpyridine complexes: their syntheses, physical properties, supramolecular constructs, and biomedical activities, *Chem. Rev*, 2008, 108: 1834-1895.
2. Sengul, A, Agac, H, Coban, B, Eroglu, E. Structural studies of complex compounds of 6, 6'-diacetyl-2,2'-bipyridine dioxime with copper(I/II), platinum(II), and palladium(II) metal ions, *Turk J Chem*, 2011, 35: 25-36.
3. Şengül, A, Arslan, H. Synthesis and Characterization of Novel Polyamide and Polyhydrazides Based on the 6,6´-disubstituted-2,2´-bipyridine, *Turk J Chem*, 2008, 32: 355-364.
4. Constable, EC. 2,2':6',2''-Terpyridines: From chemical obscurity to common supramolecular motifs, *Chem Soc Rev*, 2007, 36: 246-253.

5. Wild, A, Winter, A, Schlütter, F, Schubert, US. Advances in the field of π-conjugated 2,2′: 6′,2″-terpyridines, *Chem Soc Rev*, 2011, 40: 1459-1511.

6. Grove, LJ, Oliver, AG, Krause, JA, Connick, WB. Structure of a crystalline vapochromic platinum (II) salt, *Inorg Chem*, 2008, 47: 1408-1410.

7. Grove, LJ, Rennekamp, JM, Jude, H, Connick, WB. A new class of platinum(II) vapochromic salts, *J Am Chem Soc*, 2004, 126: 1594-1595.

8. Tam, AYY, Lam, WH, Wong, KMC, Zhu, N, Yam, VWW. Luminescent Alkynylplatinum(II) Complexes of 2, 6-Bis (N-alkylbenzimidazol-2′-yl) pyridine-Type Ligands with Ready Tunability of the Nature of the Emissive States by Solvent and Electronic Property Modulation, *Chem Eur J*, 2008, 14: 4562-4576.

9. Po, C, Tam, AY-Y, Wong, KM-C, Yam, VW-W. Supramolecular self-assembly of amphiphilic anionic platinum(II) complexes: A correlation between spectroscopic and morphological properties, *J Am Chem Soc*, 2011, 133: 12136-12143.

10. Wang, K, Haga, M-a, Monjushiro, H, Akiba, M, Sasaki, Y. Luminescent Langmuir-Blodgett Films of Platinum(II) Complex [Pt (L18) Cl](PF6)(L18= 2,6-Bis(1-octadecylbenzimidazol-2-yl) pyridine), *Inorg Chem*, 2000, 39: 4022-4028.

11. Yutaka, T, Obara, S, Ogawa, S, Nozaki, K, Ikeda, N, Ohno, T, Ishii, Y, Sakai, K, Haga, M-a. Syntheses and properties of emissive iridium (III) complexes with tridentate benzimidazole derivatives, *Inorg Chem*, 2005, 44: 4737-4746.

12. Boča, M, Jameson, RF, Linert, W. Fascinating variability in the chemistry and properties of 2, 6-bis-(benzimidazol-2-yl)-pyridine and 2, 6-bis-(benzthiazol-2-yl)-pyridine and their complexes, *Coord Chem Rev*, 2011, 255: 290-317.

13. Vaidyanathan, VG, Nair, BU. A Platinium(II)-Based Molecular Light Switch for Proteins, *Eur J Inorg Chem*, 2005, 2005: 3756-3759.

14. Muller, G, Bünzli, J-CG, Schenk, KJ, Piguet, C, Hopfgartner, G. Influence of bulky N-substituents on the formation of lanthanide triple helical complexes with a ligand derived from bis (benzimidazole) pyridine: structural and thermodynamic evidence, *Inorg Chem*, 2001, 40: 2642-2651.

15. Şengül, A, Kurt, Ö, Adler, PDF, Coles, SJ. Spectroscopic and structural properties of complexes of 3, 3′-bis (2-benzimidazolyl)-2, 2′-bipyridine with copper (I) and silver (I), *J Coord Chem*, 2014, 67: 2365-2376.

16. Cummings, SD. Platinum complexes of terpyridine: Synthesis, structure and reactivity, *Coord Chem Rev*, 2009, 253: 449-478.

17. Kaskafetou, R, Manos, MJ, Garoufis, A. Synthesis and characterization of platinum (II) oligopyridine-peptide conjugates, *Inorg Chem Commun*, 2013, 35: 176-180.

18. Aghatabay, NM, Neshat, A, Karabiyik, T, Somer, M, Haciu, D, Dülger, B. Synthesis, characterization and antimicrobial activity of Fe(II), Zn(II), Cd(II) and Hg(II) complexes with 2, 6-bis (benzimidazol-2-yl) pyridine ligand, *Eur. J. Med. Chem.*, 2007, 42: 205-213.

19. Mock, C, Puscasu, I, Rauterkus, MJ, Tallen, G, Wolff, JE, Krebs, B. Novel Pt(II) anticancer agents and their Pd (II) analogues: syntheses, crystal structures, reactions with nucleobases and cytotoxicities, *Inorg Chim Acta*, 2001, 319: 109-116.

20. Casas, JS, Castiñeiras, A, García-Martínez, E, Parajó, Y, Pérez-Parallé, ML, Sánchez-González, A, Sordo, J. Synthesis and Cytotoxicity of 2-(2′-Pyridyl)benzimidazole Complexes of Palladium(II) and Platinum(II), *Z Anorg Allg Chem*, 2005, 631: 2258-2264.

21. Gümüş, F, Pamuk, I, Özden, T, Yıldız, S, Diril, N, Öksüzoğlu, E, Gür, S, Özkul, A. Synthesis, characterization and in vitro cytotoxic, mutagenic and antimicrobial activity of platinum(II) complexes with substituted benzimidazole ligands, *J Inorg Biochem*, 2003, 94: 255-262.

22. Wang, P, Leung, CH, Ma, DL, Yan, SC, Che, CM. Structure-Based Design of Platinum(II) Complexes as c-myc Oncogene Down-Regulators and Luminescent Probes for G-Quadruplex DNA, *Chem Eur J*, 2010, 16: 6900-6911.

23. Burda, JV, Zeizinger, M, Leszczynski, J. Activation barriers and rate constants for hydration of platinum and palladium square-planar complexes: An ab initio study, *J Chem Phys*, 2004, 120: 1253-1262.

24. Largy, E, Hamon, F, Rosu, F, Gabelica, V, De Pauw, E, Guédin, A, Mergny, JL, Teulade-Fichou, MP. Tridentate N-Donor Palladium(II) Complexes as Efficient Coordinating Quadruplex DNA Binders, *Chem Eur J*, 2011, 17: 13274-13283.

25. Price, JH, Williamson, AN, Schramm, RF, Wayland, BB. Palladium(II) and platinum(II) alkyl sulfoxide complexes. Examples of sulfur-bonded, mixed sulfur-and oxygen-bonded, and totally oxygen-bonded complexes, *Inorg Chem*, 1972, 11: 1280-1284.

26. Liu, Y-J, Liang, Z-H, Li, Z-Z, Yao, J-H, Huang, H-L. Cellular uptake, cytotoxicity, apoptosis, antioxidant activity and DNA binding of polypyridyl ruthenium(II) complexes, *J Organomet Chem*, 2011, 696: 2728-2735.

27. Addison, AW, Burke, PJ. Synthesis of some imidazole-and pyrazole-derived chelating agents, *J Heterocycl Chem*, 1981, 18: 803-805.

28. Hijazi, A, Walther, ME, Besnard, C, Wenger, OS. Spectroscopy and photoredox properties of soluble platinum (II) alkynyl complexes, *Polyhedron*, 2010, 29: 857-863.

29. Braunecker, WA, Pintauer, T, Tsarevsky, NV, Kickelbick, G, Matyjaszewski, K. Towards understanding monomer coordination in atom transfer radical polymerization: synthesis of [CuI(PMDETA)(π-M)][BPh4](M= methyl acrylate, styrene, 1-octene, and methyl methacrylate) and structural studies by FT-IR and 1 H NMR spectroscopy and X-ray crystallography, *J Organomet Chem*, 2005, 690: 916-924.

30. Arslan, H, Avcı, Ç, Tutkun, B, Şengül, A. 2, 6-Bis-benzimidazolylpyridines as new catalyst in copper-based ATRP, *Polym Bull*, 2017, 74: 931-948.

31. Dey, S, Sarkar, S, Paul, H, Zangrando, E, Chattopadhyay, P. Copper(II) complex with tridentate N donor ligand: synthesis, crystal structure, reactivity and DNA binding study, *Polyhedron*, 2010, 29: 1583-1587.

32. Gayathri, V, Leelamani, E, Gowda, N, Reddy, G. Reactions of rhodium and iridium salts with multidentate N-heterocycles, *Polyhedron*, 1997, 16: 1169-1176.

33. Kose, M, McKee, V. Mn(II) complexes of a tridentate benzimidazole ligand: Synthesis, structural characterisation and catalase mimetic studies, *Polyhedron*, 2014, 75: 30-39.

34. Barton, JK, Raphael, AL. Photoactivated stereospecific cleavage of double-helical DNA by cobalt(III) complexes, *J Am Chem Soc*, 1984, 106: 2466-2468.

35. Vaidyanathan, VG, Nair, BU. Photooxidation of DNA by a cobalt(II) tridentate complex, *J Inorg Biochem*, 2003, 94: 121-126.

36. Wang, J, Shuai, L, Xiao, X, Zeng, Y, Li, Z, Matsumura-Inoue, T. Synthesis, characterization and DNA binding studies of a zinc complex with 2, 6-bis (benzimidazol-2-yl) pyridine, *J Inorg Biochem*, 2005, 99: 883-885.

37. Howe-Grant, M, Wu, KC, Bauer, WR, Lippard, SJ. Binding of platinum and palladium metallointercalation reagents and antitumor drugs to closed and open DNAs, *Biochemistry*, 1976, 15: 4339-4346.

38. Sunita, M, Anupama, B, Ushaiah, B, Kumari, CG. Synthesis, characterization, DNA binding and cleavage studies of mixed-ligand copper(II) complexes, *Arabian Journal of Chemistry*, 2014,

39. Vaidyanathan, VG, Nair, BU. Synthesis, characterization, and DNA binding studies of a chromium (III) complex containing a tridentate ligand, *Eur J Inorg Chem*, 2003, 2003: 3633-3638.

40. Vaidyanathan, VG, Nair, BU. Oxidative cleavage of DNA by tridentate copper(II) complex, *J Inorg Biochem*, 2003, 93: 271-276.

41. Vaidyanathan, V, Nair, BU. Synthesis, characterization and electrochemical studies of mixed ligand complexes of ruthenium(II) with DNA, *Dalton Trans*, 2005, 2842-2848.

42. Cusumano, M, Di Pietro, ML, Giannetto, A. Stacking surface effect in the DNA intercalation of some polypyridine platinum(II) complexes, *Inorg Chem*, 1999, 38: 1754-1758.

43. Liu, J-G, Zhang, Q-L, Shi, X-F, Ji, L-N. Interaction of [Ru(dmp)2(dppz)]2+ and [Ru(dmb)2(dppz)]2+ with DNA: effects of the ancillary ligands on the DNA-binding behaviors, *Inorg Chem*, 2001, 40: 5045-5050.

44. Ortmans, I, Elias, B, Kelly, JM, Moucheron, C, Kirsch-DeMesmaeker, A. [Ru(TAP)2(dppz)]2+: a DNA intercalating complex, which luminesces strongly in water and undergoes photo-induced proton-coupled electron transfer with guanosine-5′-monophosphate, *Dalton Trans*, 2004, 668-676.

45. Kelly, JM, Tossi, AB, McConnell, DJ, OhUigin, C. A study of the interactions of some polypyridylruthenium (II) complexes with DNA using fluorescence spectroscopy, topoisomerisation and thermal denaturation, *Nucleic Acids Res*, 1985, 13: 6017-6034.

46. Han, M-J, Duan, Z-M, Hao, Q, Zheng, S-Z, Wang, K-Z. Molecular light switches for calf thymus DNA based on three Ru (II) bipyridyl complexes with variations of heteroatoms, *J Phys Chem C*, 2007, 111: 16577-16585.

47. Zhao, J, Li, W, Ma, R, Chen, S, Ren, S, Jiang, T. Design, Synthesis and DNA Interaction Study of New Potential DNA Bis-Intercalators Based on Glucuronic Acid, *International Journal of Molecular Sciences*, 2013, 14: 16851-16865.

48. Eftink, MR, Ghiron, CA. Fluorescence quenching studies with proteins, *Anal Biochem*, 1981, 114: 199-227.

49. Yildiz, U, Coban, B. A comparative DNA binding study for heteroleptic platinum(II) complexes of pip and hpip, *Bulgarian Chem Commun*, 2016, 48: 33-38.

50. Satyanarayana, S, Dabrowiak, JC, Chaires, JB. Tris (phenanthroline) ruthenium(II) enantiomer interactions with DNA: mode and specificity of binding, *Biochemistry*, 1993, 32: 2573-2584.

51. Coban, B, Tekin, IO, Sengul, A, Yildiz, U, Kocak, I, Sevinc, N. DNA studies of newly synthesized heteroleptic platinum (II) complexes [Pt (bpy)(iip)]2+ and [Pt(bpy)(miip)]2+, *JBIC J Biol Inorg Chem*, 2016, 21: 163-175.

52. Coban, B, Yildiz, U, Sengul, A. Synthesis, characterization, and DNA binding of complexes [Pt(bpy)(pip)]2+ and [Pt(bpy)(hpip)]2+, *JBIC J Biol Inorg Chem*, 2013, 18: 461-471.

53. Grguric-Sipka, SR, Vilaplana, RA, Pérez, JM, Fuertes, MA, Alonso, C, Alvarez, Y, Sabo, TJ, González-Vílchez, F. Synthesis, characterization, interaction with DNA and cytotoxicity of the new potential antitumour drug cis-K [Ru (eddp)Cl2], *J Inorg Biochem*, 2003, 97: 215-220.

54. Reddy, PA, Santra, BK, Nethaji, M, Chakravarty, AR. Metal-assisted light-induced DNA cleavage activity of 2-(methylthio) phenylsalicylaldimine Schiff base copper (II) complexes having planar heterocyclic bases, *J Inorg Biochem*, 2004, 98: 377-386.